Bulletin of Mathematical Biology (2006) 68: 1125–1150
DOI 10.1007/s11538-006-9093-9

ORIGINAL ARTICLE

A Theoretical and Experimental Study of Competition Between Solution and Surface Receptors for Ligand in a Biacore Flow Cell

Xiaoyi He[a], Daniel Coombs[b], David G. Myszka[c], Byron Goldstein[d,*]

[a] *Computational Modeling Center, Air Products and Chemicals, Inc., 7201 Hamilton Boulevard, Allentown, PA 18195, USA*
[b] *Department of Mathematics, University of British Columbia, Vancouver, British Columbia V6T 1Z2, Canada*
[c] *Center for Biomolecular Interaction Analysis, School of Medicine, University of Utah, 50 N. Medical Drive, Room 4A417, Salt Lake City, UT 84132, USA*
[d] *Theoretical Biology and Biophysics Group, Theoretical Division, Los Alamos National Laboratory, Los Alamos, NM 87545, USA*

Received: 30 November 2005 / Accepted: 3 February 2006 / Published online: 28 June 2006

Abstract Rate constants that characterize the kinetics of binding and dissociation between biomolecules carry fundamental information about the biological processes these molecules are involved in. An instrument that is widely used to determine these rate constants is the Biacore. In a Biacore experiment, one of the reactants, which we will call the receptor, is immobilized on a sensor chip. During the binding phase of the experiment the other reactant flows past the chip. After binding, buffer alone is introduced into the flow cell and dissociation is monitored. Often surface-based binding assays are influenced by the transport of the reactant in solution, complicating the determination of the chemical rate constants from the observed binding kinetics. We propose a new way to determine the dissociation rate constant by adding soluble receptor during dissociation. The method is tested first on simulated data and then on Biacore experiments where the lac repressor protein binds and dissociates from a stretch of double stranded DNA containing the lac repressor binding site. With this method we find a dissociation rate constant $k_d = 0.075 \pm 0.005\,s^{-1}$, a value that is faster than previously obtained from Biacore experiments. In developing our method to analyze these experiments we obtain an expression for the transport limited rate constant for a Biacore experiment when soluble receptor is present during dissociation.

Keywords Surface plasmon resonance · Reaction-diffusion-advection problem · Diffusion-limited reaction · Lac repressor · Mathematical modeling

*Corresponding author.
E-mail address: bxg@t10.lanl.gov (Byron Goldstein).

1. Prologue

The work I (BG) and my colleagues present involves approximating the solution on a boundary of a time-dependent partial differential equation (PDE) with a time-dependent boundary condition by the solution to an ordinary differential equation (ODE). Imbedded in the ODE is a quantity, the transport-limited forward rate constant, obtained by solving the steady state PDE. Lee Segel was interested in this type of approximation and discussed it with me several times. This is not surprising because at the heart of this approximation is the quasi-steady state assumption (QSSA), which is an approximation that Lee championed and put on a rigorous foundation (e.g., Segel and Slemrod, 1989). On more than one occasion a colleague or a visitor to my group would show me some equation and ask me, "Under what conditions can I make a quasi-steady state approximation and how do I justify it?" I would answer,"The way I justify these approximations is simple. Lee Segel visits Los Alamos every summer. I just wait until he shows up and then I ask him." With Lee gone many things that were simple once aren't simple any more.

2. Introduction

In many settings, soluble receptors compete for ligand with receptors confined to surfaces. Soluble receptors can be produced in vivo by two different mechanisms: differential splicing and limited proteolysis (shedding) (review in Rose-John and Heinrich, 1994). The physiological roles soluble receptors play run the gamut from carrier proteins that protect ligand from degradation (Fernandex-Botran and Vitetta, 1991), to antagonists that inhibit ligand interaction with their cellular receptors (Maliszewksi, 1990; Layton, 1992), to agonists that bind ligand and associate with common signaling molecules on the surface of cells (Jones and Ross-John, 2002).

An important in vitro example of soluble receptor-surface receptor competition arises in kinetic studies of ligand–receptor dissociation when soluble receptors are used to block rebinding. A ligand is said to rebind when it dissociates from a receptor on a surface and then returns to the surface and binds another receptor rather then escaping into the bulk solution. Rebinding slows dissociation and often makes it difficult to determine the true ligand–receptor dissociation rate constant. If one uses a labeled ligand to study dissociation one can get around this problem by blocking rebinding with an excess concentration of unlabeled ligand, but in many binding studies labeled ligands are not used.

In the flow cell of the Biacore (Biacore, AB, Uppsala, Sweden), a popular optical biosensor, receptors are coupled to a flat sensor surface. Neither the ligand nor the receptor is labeled. In this instrument, through the phenomenon of surface plasmon resonance (SPR) (Garland, 1996), changes in the index of refraction caused by mass changes at the sensor surface are detected as a function of time. (For recent reviews see Rich and Myszka, 2000; Pattnaik, 2005). By continuously monitoring the SPR signal the time course of ligand–receptor binding can be followed in real time (Karlsson and Fält, 1997). Kinetic studies are carried out by

flowing ligand past the surface during the binding phase and buffer past the surface during the dissociation phase. In some cases it is observed that the dissociation kinetics speed up when the experiment is repeated at a higher buffer flow velocity indicating that transport is influencing the binding kinetics and that rebinding is occurring during dissociation.

When rebinding occurs the rate of ligand transport away from the surface is slow compared to the chemical reaction rate at the surface. To work in a regime where the opposite is the case, i.e., where transport does not influence the binding kinetics, one can, for example, lower the rate of binding by working at lower surface receptor concentrations or one can increase the rate of transport by increasing the flow rate. However, for the Biacore these approaches may not be practical since there is an upper limit to the flow rate and a lower limit to the surface receptor concentration at which a reproducible signal can be obtained. Another approach is to try to block rebinding by using a soluble receptor in the dissociation phase. When soluble receptor binds ligand it reduces the free ligand concentration. This sharpens the gradient of free ligand near the surface, thus increasing the diffusive transport away from the surface. The convective transport is also increased since, when the ligand is bound to a soluble receptor, it is transported along the flow cell and prevented from reacting with surface receptors. Of course, this method of blocking rebinding is also limited since it may not be feasible to obtain high enough concentrations of soluble receptor to block rebinding.

In this paper we derive a condition which predicts the soluble receptor concentration that is sufficient to block rebinding in a Biacore flow cell and show that it is the same condition that has been previously obtained when dissociation is from receptors on a spherical surface and transport is by diffusion alone (Goldstein et al., 1989). We also present a method for analyzing Biacore dissociation data when soluble receptor is present in the dissociation phase. The method is designed to determine the dissociation rate constant in the absence of rebinding even if the complete blocking of rebinding is not achieved at the highest soluble receptor concentration used. We first test the method on simulated data obtained from a mathematical model of a Biacore flow cell (Myszka et al., 1998) and then apply the method to Biacore dissociation studies to determine the dissociation rate constant for the lac repressor bound to a 32 base pair (bp) stretch of DNA containing the lac repressor binding site.

For those who wish to skip the mathematical details, the recipe we propose for analyzing Biacore dissociation data in the presence of soluble receptor is given in Appendix B.

3. Materials and methods

3.1. Biacore assay

The Biacore 2000 biosensor, flat carboxy-methylated sensor chip C1, NHS/EDC coupling reagents, and ethanolamine were from Biacore AB (Uppsala, Sweden). Streptavidin (Pierce) was immobilized onto a research grade C1 biosensor chip using amine-coupling chemistry (Johnson et al., 1991). The immobilization steps

were carried out at a flow rate of 20 μl/min in HEPES buffer (20 mM HEPES, 150 mM NaCl, 3.4 mM EDTA, and 0.005% P20 surfactant). All four biosensor surfaces were simultaneously activated for 7 min with a mixture of NHS (0.05 M) and EDC (0.2 M). Streptavidin was injected at a concentration of 40 mg/ml in 10 mM sodium acetate, pH 4.4, for 7 min. Ethanolamine (1 M, pH 8.5) was injected for 7 min to block any remaining activated groups. An average of 3400 response units (RU) of streptavidin was immobilized on each flow cell. A 32 bp double stranded oligo nucleotide (containing the Lac repressor binding site "LacDNA") with one strand biotinylated was captured by the streptavidin surface. Flow cells 2, 3, and 4 each contain 100, 225, and 500 RU of the lac-oligo nucleotide, respectively. Flow cell 1 was left with streptavidin only, to be used as a reference surface. (Response units are proportional to the mass at the sensor surface so the Lac repressor binding site surface concentrations for flow cells 2, 3, and 4 are in the ratio of 1:2.25:5.)

Kinetic binding experiments were performed with the instrument equilibrated at 25 °C and running at a flow rate of 100 μl/min. Lac repressor was injected over all four biosensor surfaces at a concentration of 20 nM. Immediately, following the end of the association phase, the buffer was switched to contain different concentrations of LacDNA during the dissociation phase. The LacDNA concentration varied from 50 nM to 0.85 pM with each concentration equal to 1/3 the previous concentration, i.e., 50, 16.7, 5.56 nM, and so on. All surfaces were washed with buffer containing 0.05% SDS to remove the bound protein and regenerate a fully active oligo nucleotide surface. To correct for refractive index changes and instrument noise the response data from the reference surface were subtracted from the responses obtained from the reaction surface.

3.2. Numerical methods

In simulating the flow of bound and unbound ligand in the reaction cell, we have three reaction–advection–diffusion equations, one for each species (solitary ligand, soluble receptor, and bound complex). Making the assumption that the reaction takes place approximately uniformly across the width of the flow cell we reduce the system to three coupled equations each in two dimensions. The geometry of the flow cell is such that flow will be very close to perfectly parabolic in the vertical direction. The sensor boundary is modeled by coupling three ODEs (one for each species) to the flow equations.

We solve the equations in the flow chamber using the fourth order explicit finite difference scheme outlined in Ekebjaerg and Justesen (1991) on a fixed rectangular grid. The ODE boundary condition is coupled to the flow and advanced in time using a Runge–Kutta method. Accuracy and convergence of the scheme were checked using previously existing codes (Myszka et al., 1998) and by comparing the results obtained using increasingly fine grids.

The principal numerical difficulties encountered in this work occur during the first few seconds of ligand flow and during the changeover from ligand flow to soluble receptor flow. Accurate numerical simulation of fronts is difficult to achieve using low-order methods (upwinding) and so we adopted the method used above. After the front has passed a lower order method would suffice.

3.3. Data analysis

The parameter estimates where obtained by doing nonlinear least-squares fitting of the data using software based on a finite difference, Levenberg–Marquardt algorithm. Estimates of the standard error of the parameter values were obtained using a bootstrap method (Efron and Tibshirani, 1986) where 200 simulations were performed for each estimate.

4. The full model

In this section we present a model which we solve numerically and use to test approximate results obtained in later sections. In Fig. 1 a schematic representation of a Biacore flow channel is shown during the binding phase and during a dissociation phase when soluble receptor is used to try to block rebinding. The channel has a rectangular cross section which is much wider than high. (For the standard chip, CM5, the width is 10 times the height.) For this geometry the velocity profile is constant over almost the entire width of the channel (Brody et al., 1996). Further, data is only collected in the central portion of the flow cell. We therefore need only consider concentration changes in the x and y directions.

In the flow cell one of the reactants is immobilized on a sensor chip. We call it the receptor, in analogy to a receptor on a cell surface, although it is commonly referred to as the immobilized ligand. The other reactant, called the analyte, enters at one end at a concentration C_T, flows past the sensor surface, possibly binding one or more times, and exits at the other end (Fig. 1). Along the flow cell the flow is laminar with a parabolic velocity profile such that the velocity $v(y)$ at a height y above the sensor surface is

$$v(y) = 4v_c(y/h)(1 - (y/h)) \tag{1}$$

where h is the height of the flow channel and v_c, is the flow velocity at the center of the channel ($y = h/2$). Because the velocity is zero at the sensor surface, diffusion as well as flow is important in transporting the analyte to the sensor surface.

The quantity we are interested in is the concentration of bound analyte at the sensor surface. To predict the time course of binding of analyte to receptor one

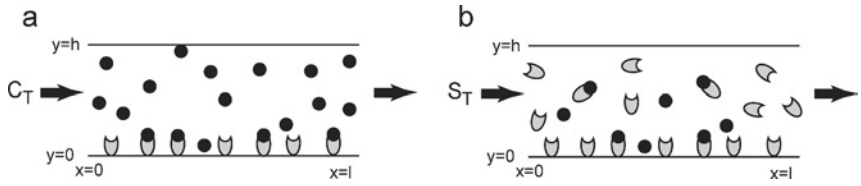

Fig. 1 Schematic diagram of a Biacore flow cell. Receptors are shown immobilized on a sensor chip on the bottom of the flow cell. (In the instrument the sensor chip is actually on the top surface.) a. In the binding phase ligand flows into the cell at concentration C_T in the absence of soluble receptor. b. In the dissociation phase the injection concentration of ligand is zero and soluble receptor is continuously injected at concentration S_T.

must be able to predict the time course of the free analyte concentration at the sensor surface. During the binding phase when soluble receptor is absent, the free analyte concentration, $C(x, y, t)$, in the flow channel obeys the following partial differential equation (Myszka et al., 1998; Mason et al., 1999):

$$\frac{\partial C}{\partial t} = D\left(\frac{\partial^2 C}{\partial x^2} + \frac{\partial^2 C}{\partial y^2}\right) - 4v_c\left(\frac{y}{h}\right)\left(1 - \left(\frac{y}{h}\right)\right)\frac{\partial C}{\partial x} \tag{2}$$

with boundary conditions:

$$\frac{\partial C(t, x, y)}{\partial y} = 0, \quad \text{at} \quad y = h \tag{3}$$

$$D\frac{\partial C(t, x, y)}{\partial y} = \frac{\partial B(t, x)}{\partial t} = k_a C(t, x, 0) R(t, x) - k_d B(t, x), \quad \text{at} \quad y = 0 \tag{4}$$

$$C(t, x, y) = C_T, \quad \text{at} \quad x = 0 \tag{5}$$

$$\frac{\partial C(t, x, y)}{\partial x} = 0, \quad \text{at} \quad x = l \tag{6}$$

$C(t, x, 0)$ is the free analyte concentration at time t and position x, at the sensor surface. $B(t, x)$ is the concentration of bound analyte-receptor complex on the cell surface and $R(t, x) = R_T - B(t, x)$ is the free surface receptor concentration. R_T is the total receptor concentration, which is constant with respect to both position and time. The rate constants for the reaction are k_a and k_d and the diffusion coefficient of the analyte is D.

At the top boundary, $y = h$, the flux vanishes because the surface is impenetrable and unreactive. At the bottom boundary, $y = 0$, the flux into the sensor surface equals the time rate of change in the amount of bound analyte at the surface. In our flow experiments we used a C1 chip with the receptors coupled directly to the sensor surface. (Usually a CM5 chip is used and receptors are attached in a 100 nm high dextran layer which is about 0.2% of the height of the flow cell. When the mean free path a ligand travels in the layer before it binds is long compared to the height of the layer, the thickness of the layer can be ignored (Goldstein et al., 1999; Mason et al., 1999). Detailed models of the effect of the dextran layer suggest that even for a C5 chip treating the surface as flat is valid under almost all experimental conditions (Edwards, 2001; Wofsy and Goldstein, 2002).

At the flow cell inlet ($x = 0$) during the binding phase the analyte concentration is constant and equal to the injection concentration, C_T. At the outlet ($x = l$), we treat the exit of analyte as if it were due entirely to flow. Although this is an approximation, since the flow is fast compared to diffusion, errors introduced by using Eq. (5) propagate in the direction of flow and so have a negligible effect on the processes occurring in the flow cell (Mason et al., 1999). At the start of the experiment we assume $B(0, x) = 0$ and $C(0, x, y) = 0$ except at the inlet.

In the dissociation phase $C_T = 0$. We assume soluble receptor is injected and that it binds analyte in solution with rate constants k_{sa} and k_{sd}. In the dissociation

phase when soluble receptor is present, Eq. (2) becomes:

$$\frac{\partial C}{\partial t} = D\left(\frac{\partial^2 C}{\partial x^2} + \frac{\partial^2 C}{\partial y^2}\right) - 4v_c\left(\frac{y}{h}\right)\left(1 - \left(\frac{y}{h}\right)\right)\frac{\partial C}{\partial x} - k_{sa}CS + k_{sd}S_c \tag{7}$$

where $S(t, x, y)$ and $S_c(t, x, y)$ are the concentrations of the free soluble receptor and the analyte-soluble receptor complex in the flow channel. The boundary conditions for C, Eqs. (3)–(6), are unchanged. The free soluble and bound receptor concentrations obey the following PDEs where D_s and D_c are the diffusion coefficients of the soluble receptor and the analyte-soluble receptor complex:

$$\frac{\partial S}{\partial t} = D_s\left(\frac{\partial^2 S}{\partial x^2} + \frac{\partial^2 S}{\partial y^2}\right) - 4v_c\left(\frac{y}{h}\right)\left(1 - \left(\frac{y}{h}\right)\right)\frac{\partial S}{\partial x} - k_{sa}CS + k_{sd}S_c \tag{8}$$

$$\frac{\partial S_c}{\partial t} = D_c\left(\frac{\partial^2 S_c}{\partial x^2} + \frac{\partial^2 S_c}{\partial y^2}\right) - 4v_c\left(\frac{y}{h}\right)\left(1 - \left(\frac{y}{h}\right)\right)\frac{\partial S_c}{\partial x} + k_{sa}CS - k_{sd}S_c. \tag{9}$$

The boundary conditions for S and S_c are:

$$\frac{\partial S(t, x, y)}{\partial y} = 0, \qquad \frac{\partial S_c(t, x, y)}{\partial y} = 0, \quad \text{at} \quad y = h \tag{10}$$

$$\frac{\partial S(t, x, y)}{\partial y} = 0, \qquad \frac{\partial S_c(t, x, y)}{\partial y} = 0, \quad \text{at} \quad y = 0 \tag{11}$$

$$S(t, x, y) = S_T, \qquad S_c(t, x, y) = 0, \quad \text{at} \quad x = 0 \tag{12}$$

$$\frac{\partial S(t, x, y)}{\partial x} = 0, \qquad \frac{\partial S_c(t, x, y)}{\partial x} = 0, \quad \text{at} \quad x = l. \tag{13}$$

The top of the flow channel is impenetrable so the flux of soluble receptor and of analyte-soluble receptor complex vanish. At the bottom boundary we assume that soluble receptor cannot react, i.e., it cannot bind to analyte that is bound to a surface receptor, so again the surface is impenetrable and the fluxes vanish.

At the flow cell inlet during the dissociation phase the analyte and the analyte-soluble receptor complex concentrations are zero and the soluble receptor concentration is constant and equal to S_T. At the outlet, as was done for the analyte flux, we take the fluxes of the soluble receptor and the analyte-soluble receptor complex equal to zero. As discussed in the Materials and Methods section, for the binding phase we solve Eq. (2) with appropriate boundary conditions, numerically. This determines the initial distribution of bound and free analyte, $C(t^*, x, y)$ and $B(t^*, x)$, at $t = t^*$, the start of the dissociation phase. Equations (7)–(9) with appropriate boundary conditions are then solved. When we simulate Biacore experiments our output is the concentration of bound receptors averaged over a central portion of the sensor surface, from $x = 0.1l$ to $x = 0.9l$.

Although we have made certain approximations, we believe the equations in this section give an excellent description of the binding kinetics in a Biacore. It should be kept in mind that even at the highest flow rates used in a Biacore (100 μl/min) one is in the low Reynolds number regime. Further, studies comparing rate constants determine from Biacore experiments at this flow rate and stopped-flow

fluorescence, a purely solution-based assay, are in excellent agreement (Day et al., 2002).

5. The transport-limited rate constant during dissociation

5.1. Obtaining an analytic expression

Rebinding to receptors on a surface will be negligible in the dissociation phase if the rate of transport away from the cell is fast compared to the chemical reaction at the surface. The maximal rate of binding to the surface will occur when all receptors are free. If R_T is the surface concentration of receptors, A is the surface area, and k_a is the forward rate constant for forming a ligand-receptor complex, then the maximal rate of binding is $k_a R_T A$. The condition that rebinding is negligible is that $k_+ \gg k_a R_T A$, where k_+ is the transport limited rate constant for dissociation. Defining the mass transport limited rate constant $k_M = k_+/A$, the nonrebinding condition becomes $k_M \gg k_a R_T$.

To obtain the transport limited rate constant for a dissociation experiment requires calculating the steady state flux away from the surface where binding occurs. The transport limited rate constant k_M is determined by the flux per unit area at the bottom surface, i.e.,

$$k_M = -\frac{D}{C_0}\frac{\partial C}{\partial y}, \quad \text{at} \quad y = 0. \tag{14}$$

(The minus sign is required since k_M is a positive quantity.)

Thus, we consider the steady state problem where $C = C_0$ on the sensor surface ($y = 0$). As discussed previously, for the cases of interest diffusion in the x-direction can be ignored since the flow is fast compared to diffusion in this direction (Mason et al., 1999). Although the flow velocity is zero at the sensor surface, diffusion in the y direction will move ligand into the flow ($y > 0$) where it can be swept along in the x direction. Since we are only interested in the analyte concentration near the sensor surface where $1 \gg (y/h)$, we ignore the quadratic term, $(y/h)^2$, in Eq. (1). Finally, we assume that during the dissociation phase only a small fraction of soluble receptors become bound so that $S \approx S_T$ and that the binding of analyte to soluble receptor can be treated as if it were irreversible. Flow velocities in Biacore experiments range from $v_c = 1$–10 cm/s but are typically 5–10 cm/s. Averaging Eq. (1) over y, the average flow velocity $\langle v \rangle = 2v_c/3$. The average time to transverse the flow cell of length $l = 0.24$ cm if $v_c = 5$ cm/s is 0.07 s. If $k_{sd} \ll 14\,\mathrm{s}^{-1}$ an analyte that binds a soluble receptor will be swept out of the flow cell before it can dissociate so the binding will appear to be irreversible. Even if this condition is not met, if the soluble receptor concentration is sufficiently high the binding will be effectively irreversible: a bound analyte molecule that dissociates from a soluble receptor quickly rebinds to another soluble receptor. Thus, we consider the following PDE where

$$0 = D\frac{\partial^2 C}{\partial y^2} - 4v_c\left(\frac{y}{h}\right)\frac{\partial C}{\partial x} - k_{sa} C S_T \tag{15}$$

at $y = 0$, $C = C_0$. We ignore the top boundary and simply require the solution to be finite at $y = \infty$. The top boundary can be ignored when the time for an analyte to diffuse from the top of the flow channel to the bottom is long compared to the time for it to traverse the length of the channel, i.e., when $l/\langle v \rangle \gg h^2/(4D)$. At $x = 0$, $C = 0$. At $x = l$ we no longer need a boundary condition because we have dropped the diffusion term in the x direction and the PDE is now first order in x.

Letting $c = C/C_0$ we write Eq. (15) in the following nondimensional form:

$$0 = \frac{\partial^2 c}{\partial y^2} - 4p\epsilon y \frac{\partial c}{\partial x} - \left(\frac{h}{\lambda}\right)^2 c \tag{16}$$

where the x and y coordinates are now scaled using the channel length, l, and channel height, h, respectively, and

$$\lambda = \sqrt{\frac{D}{k_{\mathrm{sa}} S_T}}, \quad p = \frac{v_{\mathrm{c}} h}{D}, \quad \epsilon = \frac{h}{l}. \tag{17}$$

We let

$$y_1 = (4p\epsilon)^{1/3} y, \qquad \alpha = \frac{h}{\lambda (4p\epsilon)^{1/3}} \tag{18}$$

so that Eq. (18) becomes

$$0 = \frac{\partial^2 c}{\partial y_1^2} - y_1 \frac{\partial c}{\partial x} - \alpha^2 c. \tag{19}$$

Taking the Laplace transform of Eq. (19) in x with Laplace variable s

$$0 = \frac{\partial^2 \bar{c}}{\partial y_1^2} - y_1 s \bar{c} - \alpha^2 \bar{c} \tag{20}$$

where $\bar{c}$ is the Laplace transform of c. Letting $y_2 = s^{1/3} y_1$,

$$0 = \frac{\partial^2 \bar{c}}{\partial y_2^2} - y_2 \bar{c} - \frac{\alpha^2}{s^{2/3}} \bar{c}. \tag{21}$$

Finally, letting $y_3 = y_2 + \bar{\alpha}^2 = (4p\epsilon s)^{1/3} y + \bar{\alpha}^2$, where $\bar{\alpha} = \alpha / s^{1/3}$, Eq. (21) becomes

$$0 = \frac{\partial^2 \bar{c}}{\partial y_3^2} - y_3 \bar{c}. \tag{22}$$

Equation (22) is Airy's equation which has the general solution:

$$\bar{c}(y_3) = a\,Ai(y_3) + b\,Bi(y_3) \tag{23}$$

where Ai and Bi are Airy functions, and the constants a and b are determined using the boundary conditions that $c = 1$ at $y = 0$ and $c = 0$ at $y = \infty$:

$$a = \frac{1}{s\,Ai(\bar{\alpha}^2)}, \qquad b = 0. \tag{24}$$

Thus the solution becomes

$$\bar{c} = \frac{Ai(y_3)}{s\,Ai(\bar{\alpha}^2)}. \tag{25}$$

In terms of the nondimensional variables the equation for the the transport limited rate constant, Eq. (14), becomes

$$k_{\mathrm{M}} = -\frac{D}{h}\frac{\partial c}{\partial y}, \quad \text{at} \quad y = 0. \tag{26}$$

Letting $\bar{k}_{\mathrm{M}}$ be the Laplace transform of k_{M} we have from Eqs. (25) and (26) that

$$\bar{k}_{\mathrm{M}} = -\frac{D}{h}(4p\epsilon s)^{1/3}\frac{1}{s}\frac{Ai'(\bar{\alpha}^2)}{Ai(\bar{\alpha}^2)} \tag{27}$$

where the prime indicates a derivative with respect to the argument. The Airy function and its derivative are related to modified spherical Bessel functions of the third kind K_{v} (Abramowitz and Stegun, 1964). In terms of these functions Eq. (27) becomes:

$$\bar{k}_{\mathrm{M}} = \frac{D}{h}(4p\epsilon)^{1/3}\frac{\alpha}{s}\frac{K_{2/3}(\zeta)}{K_{1/3}(\zeta)} \tag{28}$$

where $\zeta = 2\alpha^3/3s$.

To obtain an expression for k_{M} as a function of x we need to take the inverse Laplace transform of Eq. (28). Since Eq. (28) is a complicated function of s, obtaining an analytic form for its inverse Laplace transform is a formidable task. Instead, we use the following semianalytic approach. First, we express $K_{2/3}(\zeta)/K_{1/3}(\zeta)$ as a power series:

$$\frac{K_{2/3}(\zeta)}{K_{1/3}(\zeta)} = \sum_{m=1}^{\infty} a_m \zeta^{(2m-3)/3}. \tag{29}$$

Using a symbolic algebra package such as Mathematica one can easily calculate the values of the coefficients in Eq. (29). In Table 1 we list the first 20 coefficients of a_m. Substituting the expanded form of Eq. (29) into the Laplace transform of

Table 1 First 20 expansion coefficients.

m	a_m	b_m
1	0.63685e00	0.63685e00
2	0.60837e00	−0.46640e00
3	−0.16884e00	0.30446e00
4	0.77528e-1	−0.18679e00
5	−0.40009e-1	0.11053e00
6	0.21564e-1	−0.64000e-1
7	−0.11849e-1	0.36576e-1
8	0.65715e-2	−0.20738e-1
9	−0.36622e-2	0.11702e-1
10	0.20461e-2	−0.65849e-2
11	−0.11447e-2	0.36992e-2
12	0.64093e-3	−0.20760e-2
13	−0.35901e-3	0.11644e-2
14	0.20114e-3	−0.65287e-3
15	−0.11271e-3	0.36599e-3
16	0.63160e-4	−0.20515e-3
17	−0.35395e-4	0.11498e-3
18	0.19836e-4	−0.64445e-4
19	−0.11117e-4	0.36119e-4
20	0.62303e-5	−0.20243e-4

$a_m = b_m = 2^{1/3}\frac{\Gamma(2/3)}{\Gamma(1/3)}$.
a_m is defined by Eq. (29) in the text and b_m is defined by Eq. (A.10) in Appendix A.

$\bar{k}_{\mathrm{M}}$, Eq. (28), we have

$$\bar{k}_{\mathrm{M}} = \frac{D}{h}(4p\epsilon)^{1/3}\alpha \sum_{m=1}^{\infty} a_m \left(\frac{2\alpha^3}{3}\right)^{(2m-3)/3} s^{-2m/3}. \tag{30}$$

We now obtain $k_{\mathrm{M}}(x)$ by taking the inverse Laplace transform of Eq. (30):

$$k_{\mathrm{M}} = \frac{D}{h}(4p\epsilon)^{1/3}\alpha \sum_{m=1}^{\infty} \frac{a_m}{\Gamma(2m/3)} \left(\frac{2\alpha^3}{3}\right)^{(2m-3)/3} x^{(2m-3)/3}. \tag{31}$$

From Eq. (31) we obtain k_{M}, the transport limited rate constant averaged over the sensor surface:

$$\langle k_{\mathrm{M}} \rangle = \int_0^1 k_{\mathrm{M}}\, \mathrm{d}x = \frac{D}{h}(4p\epsilon)^{1/3}\alpha \sum_{m=1}^{\infty} \frac{a_m}{\Gamma((2m+3)/3)} \left(\frac{2\alpha^3}{3}\right)^{(2m-3)/3}. \tag{32}$$

In Appendix A, for completeness, we derive an expression for $\langle k_{\mathrm{M}} \rangle$ for the forward kinetics when both ligand and soluble receptor are continuously injected. During the binding phase the presence of soluble receptor will slow transport of the ligand to the sensor surface and $\langle k_{\mathrm{M}} \rangle$ will be a decreasing function of the soluble receptor concentration. This is just the opposite of what we have seen for the dissociation phase.

5.2. Limiting behavior of the transport-limited rate constant

We consider two limits, when the soluble receptor concentration $S_T = 0$ ($\alpha = 0$) and when $S_T = \infty$ ($\alpha = \infty$). When $\alpha = 0$ the only nonzero term in Eq. (31) is the $m = 1$ term. From Eq. (29) and pp. 446–447 of Abramowitz and Stegun (1964) we have that

$$a_1 = \lim_{\zeta \to 0} \zeta^{1/3} \frac{K_{2/3}(\zeta)}{K_{1/3}(\zeta)} = -(2/3)^{1/3} \frac{Ai'(0)}{Ai(0)} = \frac{2^{1/3}\Gamma(2/3)}{\Gamma(1/3)}.$$

Returning to dimensional units where x in the equation below is now a length along the sensor surface, we have that when $S_T = 0$

$$k_m(x) = \frac{D}{h}(4p\epsilon)^{1/3} \frac{a_1}{\Gamma(2/3)} \left(\frac{2}{3}\right)^{-1/3} = \frac{3^{1/3}}{\Gamma(1/3)} \left(\frac{4v_c D^2}{xh}\right)^{1/3} \tag{33}$$

and we recover the result of Lok et al. (1983). Averaging over x we have that

$$\langle k_M \rangle = \frac{3}{\Gamma(1/3)} \left(\frac{3v_c D^2}{2lh}\right)^{1/3} \approx 1.282 \left(\frac{v_c D^2}{lh}\right)^{1/3}. \tag{34}$$

To obtain the limit as $S_T \to \infty$ ($\alpha \to \infty$) it is simplest to return to Eq. (27). In this limit $Ai'(\bar{\alpha}^2)/Ai(\bar{\alpha}^2) = -\bar{\alpha} = -\alpha/s^{1/3}$. Substituting this expression into Eq. (27) and taking the inverse transform we find that in the limit that $S_T \to \infty$

$$k_M = \langle k_M \rangle = \sqrt{k_{sa} S_T D}. \tag{35}$$

As discussed in the beginning of this section, soluble receptor will effectively block rebinding when $k_M \gg k_a R_T$. From Eq. (35) this condition becomes

$$S_T \gg (k_a R_T)^2 / D k_{sa}. \tag{36}$$

If $k_a = k_{sa}$, an instructive way to write this inequality is $S_T \gg R_T/\lambda$ where λ is given by Eq. (17). In this form we see that for competing with soluble receptors, the surface receptor concentration R_T has an effective three-dimensional concentration equal to the surface concentration divided by the mean free path a ligand travels in solution before binding to a soluble receptor. Except for a constant, Eq. (36) is the same as for the case when soluble receptors compete for dissociating ligand with cell surface receptors in the absence of flow (Goldstein et al., 1989, 1999).

5.3. Approximate expression for the transport-limited rate constant

In analyzing dissociation data we will find it useful to have a simple accurate expression for $\langle k_M \rangle$. We accomplish this by writing $\langle k_M \rangle$ as a Padé approximant that has the appropriate limits at $S_T = 0$, Eq. (34), and $S_T = \infty$, Eq. (35). We use the

following expression which has these limits:

$$\langle k_{\mathrm{M}}(S_{\mathrm{T}})\rangle = \langle k_{\mathrm{M}}(0)\rangle \frac{g(\alpha)}{0.807594} \tag{37}$$

where α is given by Eq. (18) and

$$g(\alpha) = \frac{0.807594 + p_1\alpha + p_2\alpha^2 + p_3\alpha^3 + \alpha^4}{1 + p_4\alpha + p_5\alpha^2 + \alpha^3}. \tag{38}$$

From Eq. (32) we have that

$$g(\alpha) = \alpha \sum_{m=1}^{\infty} \frac{a_m}{\Gamma\left((2m+3)/3\right)} \left(\frac{2\alpha^3}{3}\right)^{(2m-3)/3}. \tag{39}$$

The constant $3(3/8)^{1/3}/\Gamma(1/3) \approx 0.807594$ in $g(\alpha)$ is chosen to give the correct limit as $S_{\mathrm{T}} \to \infty$ and therefore $\alpha \to \infty$.

We obtain the values of p_1 through p_5 in Eq. (39) by carrying out a nonlinear-least squares fit of the above expression to numerical values obtained from Eq. (39). The fit is shown in Fig. 2a. In Fig. 2b we show that the absolute value of the deviation is never greater than 0.06%. Note that $\alpha \propto \sqrt{S_{\mathrm{T}}}$ and in the limit that $S_{\mathrm{T}} = \infty$, $g(\alpha) = \alpha$, i.e., for large values of the soluble receptor concentration, $\langle k_{\mathrm{M}}\rangle$ goes as $\sqrt{S_{\mathrm{T}}}$. One sees in Fig. 2 that $g(\alpha) \approx \alpha$ for $\alpha \geq 2$. For example, when $\alpha = 2$, $g(\alpha) = 2.0622$.

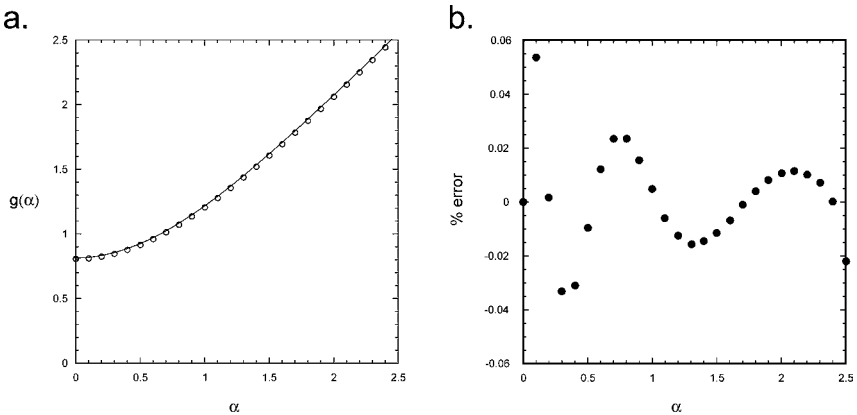

Fig. 2 The Padé approximant to the function $g(\alpha)$. a. The function $g(\alpha)$ is calculated from Eq. (39) (*open circles*) and the fit to these calculated values of the Padé approximant give by Eq. (38) (*solid line*) where $p_1 = 1.24240$, $p_2 = 1.41371$, $p_3 = 1.045663$, $p_4 = 1.55924$, and $p_5 = 1.00918$. b. The percent deviation of the Padé approximant from Eq. (39). The absolute value of the deviation is always less than 0.06% of the value calculated from Eq. (38).

6. The halflife for dissociation

6.1. A simple expression for the halflife for dissociation

Our aim is to present a method to obtain the dissociation rate constant, k_a, from Biacore dissociation experiments when soluble receptor is present to inhibit rebinding during dissociation. We start by obtaining an analytic expression for $t_{1/2}$, the half-life of dissociation, that accurately predicts the values of the half-life of dissociation when the ratio of the rate of reaction to the rate of transport, δ, is small.

A simple way to describe the kinetics of dissociation when transport effects binding is by an ODE of the same form as the chemical rate equation for a well mixed system, but with the rate constants replaced by effective rate coefficients, Eq. (40) below. (This is sometimes referred to as the effective rate constant (ERC) model (Edwards, 2004)). These rate coefficients are functions of the free receptor concentration and thus, vary in time (reviewed in Goldstein and Dembo, 1995; Goldstein et al., 1999; Mason et al., 1999). For example, the dissociation rate coefficient attempts to capture the following process: as ligands dissociate receptors become free and the probability increases that a ligand that dissociates from one receptor will rebind to another receptor on the sensor surface and slow the observed dissociation. The quality of the ERC approach has been analyzed by Edwards (2004) who formally showed that it gives good estimates of the rate constants, k_a and k_d when the ratio of the rate of reaction to the rate of transport is small, i.e., when $\delta < 1$.

$$\frac{\mathrm{d}B}{\mathrm{d}t} = \frac{k_a}{1 + k_a(R_T - B)/\langle k_M \rangle} C_T(R_T - B) - \frac{k_d}{1 + k_a(R_T - B)/\langle k_M \rangle} B. \tag{40}$$

One can solve Eq. (40) to obtain a transcendental equation for the fraction of bound receptors remaining at time t after the dissociation phase has begun. At the start of dissociation, $t = 0$ and the concentration of bound receptors is $B(0)$. Since during dissociation $C_T = 0$, we have that

$$(1 + \delta) \ln b - \delta \bar{b}(b - 1) = -k_d t \tag{41}$$

where

$$b(t) = B(t)/B(0), \quad \delta = k_a R_T/\langle k_M \rangle, \quad b_0 = B(0)/R_T. \tag{42}$$

(In the absence of soluble ligand $\delta \approx 0.78 Da$, where Da is the Damköhler number.) To express δ as a function of the soluble ligand concentration we use Eqs. (37) and (38). From Eq. (41) the halflife for dissociation is

$$t_{1/2} = \frac{\ln 2}{k_d}(1 + \delta(1 - b_0/(2 \ln 2))). \tag{43}$$

6.2. *Adding a correction term to the halflife for dissociation*

In Fig. 3 we show a series of simulated Biacore experiments obtained by numerically solving the set of PDEs that comprise the full model (Eqs. (7)–(10)). The four sets of simulations are for four different concentrations of receptors on the Biacore sensor surface. The ligand concentration is the same in all simulations during the binding phase. For each receptor concentration seven simulations are shown corresponding to seven different concentrations of soluble receptor in the dissociation phase. To properly test whether we can obtain accurate estimates of k_d when rebinding is high we have chosen a forward rate constant,

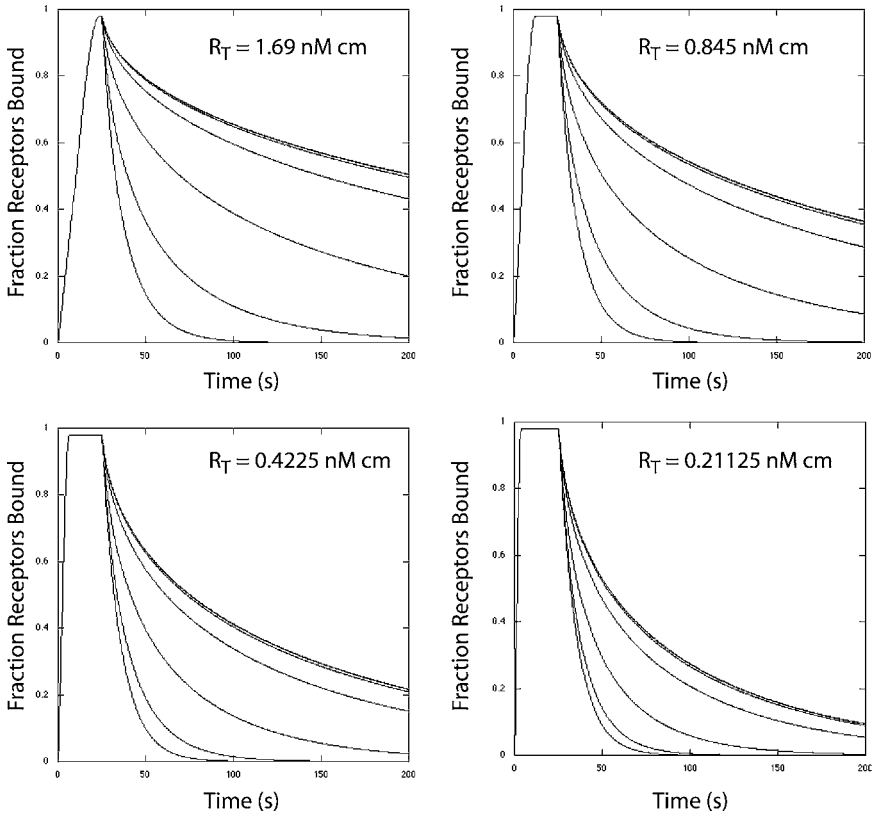

Fig. 3 Simulation of biacore binding and dissociation experiments for four different receptor concentrations (R_T) on the sensor surface. The ligand concentration in the binding phase is the same in all simulations ($C_T = 5 \times 10^{-8}$ M). In the dissociation phase the soluble receptor concentrations were $S = 0$ nM, 1 nM, 10 nM, 100 nM, 1 μM, 10 μM and 100 μM. The $S = 0$ and 1 nM are indistinguishable in these plots. The simulations were done using a 175×175 grid with the following parameters: $k_a = k_{as} = 1 \times 10^8\,\mathrm{M^{-1}\,s^{-1}}$, $k_d = k_{sd} = 0.10\,\mathrm{s^{-1}}$, $l = 0.24$ cm, $h = 0.005$ cm, $v_c = 10$ cm/s, and $D = D_s = D_c = 1 \times 10^{-6}\,\mathrm{cm^2/s}$. In all cases the binding went to equilibrium ($b_0 = 0.9804$) before the start of the dissociation phase at $t = 25$ s. The $t_{1/2}$ values for dissociation ($b = 0.4902$) were obtained from the numerical results used to plot these curves and are given in Table 1.

$k_a = 1 \times 10^8\,\mathrm{M^{-1}\,s^{-1}}$, and receptor concentrations that give substantial rebinding. For the four receptor concentrations, in the absence of soluble ligand during dissociation $\delta = k_a R_T/\langle k_M\rangle$=65.0 ($R_T = 1.69\,\mathrm{nM\,cm}$), 32.5 ($R_T = 0.845\,\mathrm{nM\,cm}$), 16.3 ($R_T = 0.4225\,\mathrm{nM\,cm}$) and 8.2 ($R_T = 0.21125\,\mathrm{nM\,cm}$). In the simulations $k_d = 0.1\,\mathrm{s^{-1}}$ which, in the absence of rebinding, corresponds to a halflife of 6.9 s. From our simulations we see that when $S = 0$ and $R_T = 1.69\,\mathrm{nM\,cm}$, $t_{1/2} = 189.1$ s, and rebinding slows dissociation more than 20-fold.

In Table 2 we present the $t_{1/2}$ values from Fig. 3 and their predicted values from Eq. (43). We see that the percent error in the predicted values are always less than 30%. Since the theory is expected to be accurate only for $\delta < 1$ (Edwards, 2004) this is not surprising. However, the question we are interested in is: can we use Eq. (43) to obtain an accurate estimate of k_d, the intrinsic dissociation constant?

Before answering this question we note that Eq. (43) predicts that $t_{1/2}$ is only a function of δ and b_0. In all the simulations in Fig. 3 equilibrium is reached before the onset of dissociation so b_0 is the same for all simulated dissociation

Table 2 Halflife for dissociation in the presence of soluble receptor (S) from simulated experiments in Fig. 3, $t_{1/2}$(sim), and as predicted by Eq. (43), $t_{1/2}$(Eq. (43)).

R_T (nM cm)	S	δ	$t_{1/2}$ (Eq. (43))	$t_{1/2}$ (sim)	% difference
1.69	0	65.022	138.89	189.13	0.26560
	1 nM	64.716	138.27	188.37	0.26597
	10 nM	61.747	132.25	181.06	0.26960
	100 nM	43.995	96.221	131.75	0.26967
	1 μM	16.752	40.930	47.000	0.12916
	10 μM	5.3320	17.753	15.125	−0.17375
	100 μM	1.6883	10.358	8.0900	−0.28033
0.845	0	32.511	72.913	98.200	0.25751
	1 nM	32.358	72.600	97.800	0.25767
	10 nM	30.874	69.590	94.000	0.25968
	100 nM	21.576	51.570	69.500	0.25799
	1 μM	8.3759	23.931	26.940	0.11171
	10 μM	2.6660	12.342	11.060	−0.11593
	100 μM	0.84414	8.6447	7.5300	−0.14803
0.4225	0	16.256	39.922	52.625	0.24138
	1 nM	16.179	39.767	52.500	0.24254
	10 nM	15.437	38.261	50.750	0.24610
	100 nM	10.999	29.254	38.375	0.23769
	1 μM	4.1880	15.431	17.000	0.092294
	10 μM	1.3330	9.6368	9.0190	−0.068502
	100 μM	0.42207	7.7881	7.2500	−0.074217
0.21125	0	8.1662	23.505	29.940	0.21493
	1 nM	8.1278	23.427	29.830	0.21465
	10 nM	7.7549	22.670	28.910	0.21584
	100 nM	5.5255	18.146	22.670	0.19958
	1 μM	2.1039	11.201	12.000	0.066558
	10 μM	0.66966	8.2906	8.0000	−0.036319
	100 μM	0.21203	7.3618	7.1100	−0.035415

Note. R_T is the concentration of receptors on the sensor surface, $\delta = k_a R_T/\langle k_M\rangle$ is a measure of the competition between binding and transport, and the % difference =($t_{1/2}$(sim)-$t_{1/2}$(Eq. (43))/$t_{1/2}$(sim).

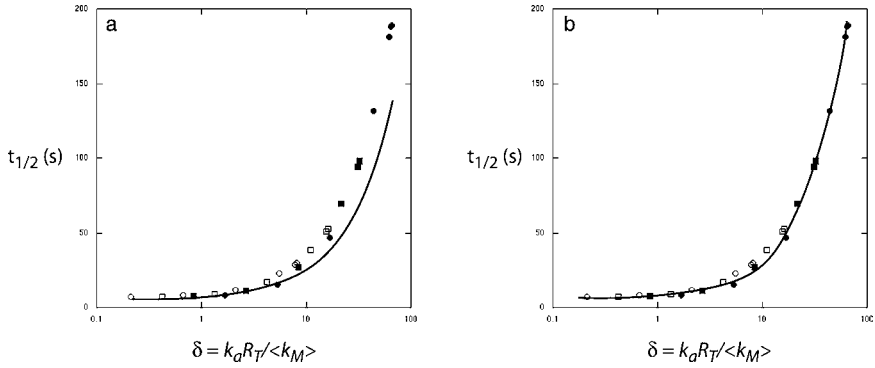

Fig. 4 The halflife for dissociation versus $\delta = k_a R_T/\langle k_M \rangle$. In both panels the symbols indicate the halflives for dissociation as calculated from the simulated experiments in Fig. 3, given in Table 2. a. The solid line is a nonlinear least squares fit of Eq. (43) to the half-lives. b. The solid line is a nonlinear least squares fit of Eq. (44) to the half-lives. The free parameters were determined to be: $c_1 = 9.55924 \times 10^{-3}$, $c_2 = -2.41944 \times 10^{-4}$ and $c_3 = 1.87714 \times 10^{-6}$. The correction term in Eq. (44) is negligible for $\delta \leq 1$. At $\delta = 1$ it equals 0.0093 while, $1 + \delta(1 - b_0/2 \ln 2)$, it is bounded between 1.28 and 2.0.

experiments. In Fig. 4a we plot the $t_{1/2}$ values of the simulated experiments (Table 2) and see that $t_{1/2}$ appears to be only a function of δ for the full model, although it may depend weakly on R_T as well. (We have not determined as yet if the "scatter" in the plot of $t_{1/2}$ versus δ is because $t_{1/2}$ is a function of both δ and R_T, or because of numerical error.) Also shown in Fig. 4a is $t_{1/2}$ calculated from Eq. (43).

That $t_{1/2}$ can be approximated as a function of δ suggests that Eq. (43) can be improved by adding a correction term that is only a function of δ. We do this by taking as our expression for $t_{1/2}$

$$t_{1/2} = \frac{\ln 2}{k_d}(1 + \delta(1 - b_0/(2 \ln 2)) + c_1\delta^2 + c_2\delta^3 + c_3\delta^4) \tag{44}$$

where c_1, c_2 and c_3 are determined by fitting Eq. (44) to the simulated results as shown in Fig. 4b. These parameters are then held fixed at their determined values when we fit our experimental data. Note that if $t_{1/2}$ can be taken to be only a function of δ, then the parameters c_1, c_2 and c_3 will be the same for all Biacore experiments. Indeed, in Fig. 4b their values were determined by fitting simulations corresponding to four different receptor concentrations.

6.3. Comparison with simulated data

We have now assembled the elements necessary to fit dissociation data, $t_{1/2}$ values as a function of soluble receptor concentration, and obtain an estimate of the intrinsic dissociation rate constant, k_d (summarized in Appendix B). As our fitting function we use Eq. (44) with the parameters c_1 through c_3 given in the figure

caption of Fig. 4 and δ given below.

$$\delta = \frac{k_a R_T}{\langle k_M \rangle} = \frac{\bar{\delta}}{g(\bar{\alpha}(S_T^{1/2})} \quad \text{and} \quad \alpha = \bar{\alpha}(S_T/S_0)^{1/2}. \tag{45}$$

The quantity $g(\alpha)$ is given by Eq. (38) with the parameters p_1 through p_5 given in the figure caption of Fig. 2. We take the lumped parameters $\bar{\delta}$ and $\bar{\alpha}$ as free parameters in our fits. In terms of the parameters of the model

$$\bar{\delta} = \frac{0.80759 k_a R_T}{\langle k_M(0) \rangle}, \qquad \bar{\alpha} = \frac{h}{(4p\epsilon)^{1/3}} \left(\frac{k_{sa} S_0}{D}\right)^{1/2} \tag{46}$$

where we will take $S_0 = 1$ nM. Both parameters are dimensionless with $\bar{\alpha}$ being the value of α when $S_T = 1$ nM. 5

In fitting data we take as free parameters k_d, b_0, $\bar{\alpha}$ and $\bar{\delta}$ corresponding to the experiment with the largest surface receptor concentration. In addition there are eight fixed parameters, p_1 through p_5 and c_1 through c_3. Shown in Fig. 5 are

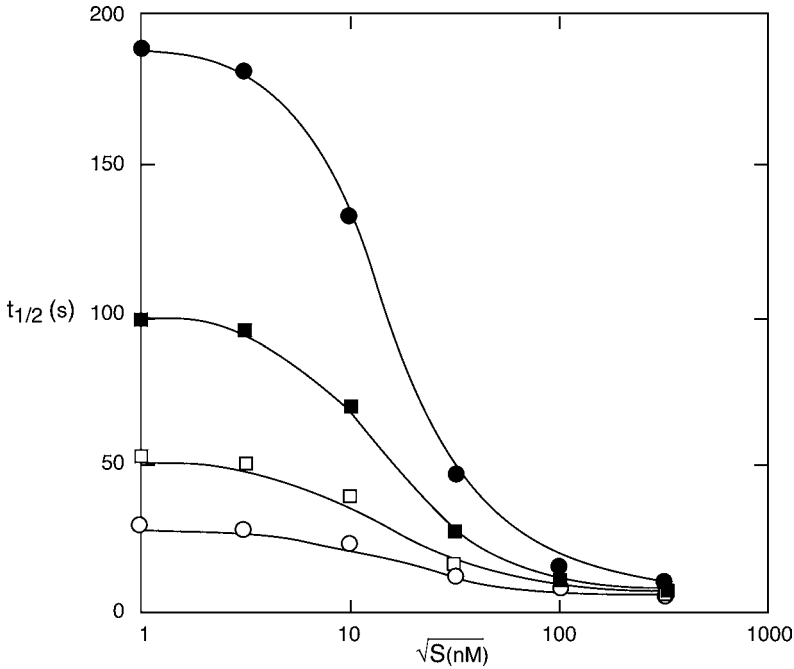

Fig. 5 Nonlinear-least-squares fits using Eq. (44) to fit the halflives for dissociation as a function of S_T from the simulations in Fig. 3. S_T is the soluble receptor concentration injected in the dissociation phase. The four curves, corresponding to the four surface receptor concentrations at which the simulations were done, were fit simultaneously. The S_T and $t_{1/2}$ values are given in Table 2. The best fit values of the parameters are: $k_d = 0.104 \pm 0.011\ s^{-1}$, $\bar{\alpha} = 0.101 \pm 0.002$, $\bar{\delta} = 41.7 \pm 5.5$, and $b_0 = 0.802 \pm 1.00$. The exact values from the parameters used in the simulations are: $k_d = 0.100\ s^{-1}$, $\bar{\alpha} = 0.098259$, $\bar{\delta} = 52.51$ and $b_0 = 0.98039$.

simultaneous fits of the $t_{1/2}$ values from the four sets of simulated experiment in Fig. 3. We are able to recover accurate values for k_d and $\bar{\alpha}$ (fit values: $0.103\,s^{-1}$ and 0.101; exact values: $0.100\,s^{-1}$ and 0.098), a somewhat less accurate value for δ (fit value: 41.7; exact value: 52.5) and a totally unreliable value for b_0. To make an accurate estimate of $\bar{\alpha}$ requires data that varies over a large range of S values. In the simulations S varies over five orders of magnitude. To make an accurate estimate of δ requires a large variation in R_T. In the simulations R_T varies eight fold. The predicted value of $t_{1/2}$ is relatively insensitive to the parameter b_0 which enters Eq. (44) in the factor $(1 - b_0/(2\ln 2))$ and can vary only between 0.28 and 1.0. The most important point however, is that Eq. (44) can be used to get a good estimate of the intrinsic dissociation rate constant.

7. Dissociation of the lac repressor

To determine the rate constant for dissociation of the lac repressor from double stranded DNA containing the lac repressor binding site, lac repressor was injected over four biosensor surfaces, one devoid of DNA (the control) and three with different concentrations of DNA coupled to their surfaces (Fig. 6). In the dissociation phase DNA was injected to block rebinding. The experiments show that in the absence of soluble receptor and even at the lowest surface receptor concentration, rebinding does occur and transport does influence the binding kinetics. If transport were fast compared to binding the dissociation kinetics would be independent of the presence of soluble receptor, i.e., there would be no competition between surface and solution DNA for dissociated lac repressor protein.

Figure 7 shows the values of $t_{1/2}$ as a function of soluble DNA from the experiments in Fig. 6 and the fits to these data using Eq. (44). For the highest density surface, 500 RU, we find $\bar{\delta} = 14.2 \pm 4.72$ which from Eq. (46) corresponds

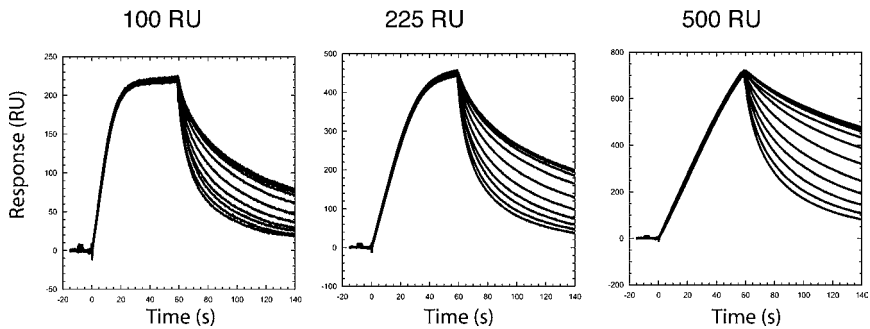

Fig. 6 Biacore experiments where double stranded DNA containing the lac repressor binding site was immobilized at three different densities, 100, 225 and 500 RU. Lac repressor protein was injected at 44 nM for 60 s, followed by an injection of double stranded DNA containing the lac repressor binding site at a flow rate of 100 μl/min. The concentrations of DNA during dissociation were 0 nM (3 experiments), 0.00254, 0.00762, 0.0229, 0.0686, 0.206, 0.617, 1.85, 5.56, 16.7, and 50 nM.

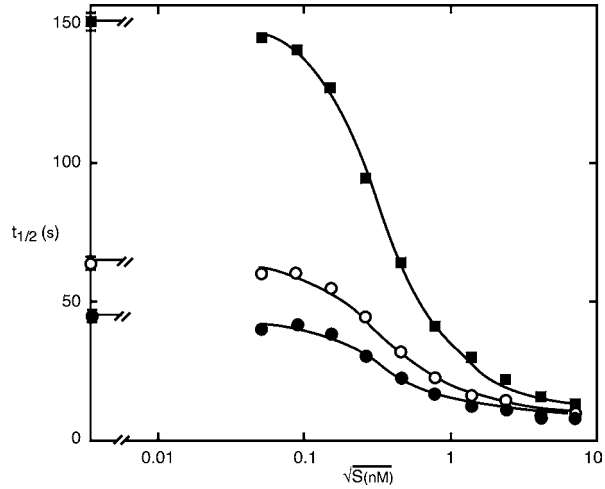

Fig. 7 Determining the dissociation rate constant for the lac repressor, k_d, from dissociation experiments in the presence of soluble receptor, S. the halflives for dissociation, $t_{1/2}$, were determined from the data shown in Fig. 6 by fitting Eq. (43) to each dissociation curve separately. Eq. (44) was then used to simultaneously fit these data. The best fit values of these parameters are: $k_d = 0.075 \pm 0.005\,s^{-1}$, $\bar{\alpha} = 4.10 \pm 0.09$, $\bar{\delta} = 14.2 \pm 4.7$. In addition the three values of b_0 for the three surface concentrations were taken as free parameters but the fits were insensitive to the values of these parameters providing b_0 was kept between zero and one.

to $\delta = 17.6$. Therefore $\delta = 3.5$ at the lowest density surface, 100 RU. Since $\delta > 1$, this indicates that for all three sensor surfaces substantial rebinding occurred during dissociation.

We find that $k_d = 0.075 \pm 0.005\ s^{-1}$. Bondeson et al. (1993) used a Biacore experiment to analyze the kinetics of binding and dissociation of lac repressor-DNA and found $k_a = 1.8 \times 10^6\,M^{-1}\,s^{-1}$ and $k_d = 3.4 \times 10^{-4}\,s^{-1}$, a value that is more than 200 times slower than the value we obtain. In analyzing their dissociation data to obtain k_d they noted that dissociation appears to be biphasic with the faster first phase having a $k_d > 2 \times 10^{-3}\,s^{-1}$. They suggest that the biphasic behavior may be due to heterogeneity in the DNA coupled to the sensor surface. An alternate possibility is that rebinding is slowing dissociation. At short times dissociation is faster since most receptors on the sensor surface are bound. With time, receptors become free, rebinding increases and dissociation slows. If this is the explanation than in addition to underestimating k_d, they will have underestimated k_a as well. Goeddel et al. (1977) used a membrane filter assay (Yansura et al., 1977) and found $k_d = 0.01$–$0.08\,s^{-1}$ for dissociation of the lac repressor from 21 and 26 bp lac operators over a wide range of salt concentrations. In this assay rebinding was blocked. The forward rate constant was found to be more sensitive to salt concentration than the dissociation rate possibly because long-range electrostatic forces may accelerate association. Goeddel et al. (1977) also determined k_a values in the range of 10^8–$10^9\,M^{-1}\,s^{-1}$, again much faster than those determined by Bondeson et al. (1993).

8. Discussion

One of the major uses of the Biacore is to obtain accurate estimates of rate constants. The binding kinetics in the flow cell of a Biacore are influenced by the transport of the ligand about the sensor surface by flow and diffusion, and by the chemical reaction at the surface which is described by the binding and dissociation rate constants, k_a and k_d. Under certain conditions transport can influence the binding kinetics and make it difficult to obtain accurate estimates of these rate constants. The influence of transport can be detected by carrying out experiments at different flow velocities or different densities of receptors on the sensor surface. For example, if the rate of dissociation increases when the flow velocity is increased or when the receptor density is decreased, it is a strong indication that transport is influencing the binding kinetics. Another tool to detect transport effects during dissociation is to inject soluble receptor in the dissociation phase. If the presence of soluble receptor speeds dissociation than rebinding is occurring and slowing dissociation. Further, if rebinding is occurring, i.e., if transport is too slow to sweep ligand that has dissociated out of the flow cell before it returns to the surface and binds again, than transport is also slowing the forward kinetics.

We have proposed a way to obtain improved estimates of dissociation rate constants from Biacore experiments when rebinding occurs during dissociation. We tested the method both on simulated data and by analyzing the dissociation of the lac repressor protein from its binding site on double stranded DNA. Our method proposes a series of experiments using a range of soluble receptor concentrations during the dissociation phase (see Fig. 6). Of course, if high enough soluble receptor concentrations can be achieved then dissociation becomes independent of the soluble receptor concentration and no new theory is necessary for simple reactions: the intrinsic off rate constant $k_d = \ln(2)/t_{1/2}$, and the dissociation is described by a single exponential. In kinetic experiments it is often difficult to obtain high enough soluble receptor concentrations to effectively compete with surface receptors (see Eq. (36)). The method we have proposed allows one to determine k_d using lower soluble receptor concentrations.

We started by obtaining an expression for the transport limited rate constant, $\langle k_M \rangle$, for a dissociation experiment in which soluble ligand was present. The expression we obtained, Eq. (32), involved an infinite sum and was unwieldy to use in analyzing experimental data. We therefore obtained an approximate expression for $\langle k_M \rangle$ given by Eqs. (37) and (38), that had the correct limiting behavior and that was highly accurate for all soluble receptor concentrations. We then considered a model which describes the kinetics of dissociation in terms of an ODE rather than a PDE, where to account for transport effects, k_d is replaced by a time dependent rate coefficient involving $\langle k_M \rangle$ (Eq. (40) with $C_T = 0$). This led to a simple analytic expression for $t_{1/2}$, Eq. (43). Unfortunately, when rebinding was high, i.e., when $\delta > 1$, the expression was inaccurate and predicted halflives that were in error by as much as 30% when compared with simulated data obtained by solving the full PDE model. (Recall that $\delta = k_a R_T / \langle k_M \rangle$ is a measure of the rate of rebinding to the rate of transport.) However, we observed from our simulated data that $t_{1/2}$ was to a good approximation a function only of δ (see Fig. 4), at least for $\delta \leq 65$. (The upper limit comes about because we did not simulate experiments with higher δ values

than 65 but there is no reason to think that the result won't hold for higher values of δ as well.) This suggested we could improve the accuracy of our expression for $t_{1/2}$ by adding a correction term which was only a function of δ. Using the new expression for $t_{1/2}$, Eq. (44), to fit values of $t_{1/2}$ from our simulations for different values of S (Fig. 5), we were able to recover the k_d value used in the simulations. We then used Eq. (44) to fit Biacore data to determine k_d for the dissociation of the lac repressor from a 32 bp string of double stranded DNA that contained the lac repressor binding site and obtained a value for $k_d = 0.075 \pm 0.005\,s^{-1}$ which was considerably faster than the value previously obtaining by Bondeson et al. (1993) from Biacore experiments. The addition in the dissociation phase of soluble DNA containing the lac repressor binding site increased the rate of dissociation (Fig. 6) and demonstrated that transport was strongly influencing the binding kinetics. One possible explanation for the difference between our value for k_d and that determined by Bondeson et al. is that in their experiments as in ours, rebinding substantially slowed dissociation.

Acknowledgements

This work was supported by NIH grant R37 GM35556, NSF grant DBI-0352341 and performed in part by the Department of Energy through contract W-7405-ENG-36.

Appendix A: $\langle k_M \rangle$ during the association phase

We calculate the transport limited forward rate constant during the binding phase of a Biacore experiment when ligand and soluble receptor are continuously injected into the flow cell. For the association phase we wish to calculate the flux into the sensor surface so we set up a steady state problem where at $y = 0$, $C = 0$ and at $y = \infty$, $C = C_0$. In Eq. (19), $c = C/C_0$ so at $y = \infty$, $c = 1$. The Laplace transform of Eq. (19) in x with Laplace variable s is

$$0 = \frac{\partial^2 \bar{c}}{\partial y_1^2} - y_1(s\bar{c} - 1) - \alpha^2 \bar{c} \tag{A.1}$$

where $\bar{c}$ is the Laplace transform of c. This eqnarray differs from that for the dissociation case because of the additional c_0 in the second term of Eq. (A.1). This term arises because $c = c_0$ at $x = 0$. Introducing the following quantities:

$$Z = \frac{s}{\pi \bar{\alpha}^2}\left(\bar{c} - \frac{1}{s}\right), \tag{A.2}$$

and

$$y_3 = s^{1/3} y_1 + \bar{\alpha}^2, \tag{A.3}$$

Eq. (A.1) becomes:

$$\frac{1}{\pi} = \frac{\partial^2 Z}{\partial y_3^2} - y_3 Z. \tag{A.4}$$

Equation (A.4) has the specific solution (Abramowitz and Stegun, 1964) $Z = Hi(y_3)$, so that the complete solution can be written in the form

$$\bar{c} = a\,Ai(y_3) + b\,Bi(y_3) + Hi(y_3), \tag{A.5}$$

For the association problem, we have $c = 0$ at $y = 0$ and $c = c_0$ at $y = \infty$. These boundary conditions lead to:

$$a = -\frac{1}{Ai(\bar{\alpha}^2)}\left[\frac{1}{\pi\bar{\alpha}^2} + Hi(\bar{\alpha}^2) - Bi(\bar{\alpha}^2)\right], \quad b = -1 \tag{A.6}$$

and the solution becomes:

$$\bar{c} = \frac{1}{s} - \frac{\pi\bar{\alpha}^2}{s}\left[\frac{Ai(y_3)}{Ai(\bar{\alpha}^2)}\left[\frac{1}{\pi\bar{\alpha}^2} + Hi(\bar{\alpha}^2) - Bi(\bar{\alpha}^2)\right] - Hi(y_3) + Bi(y_3)\right]. \tag{A.7}$$

We can now use Eq. (A.7) to calculate k_M from Eq. (24). Letting $\bar{k}_M$ be the Laplace transform of k_M it follows that

$$\bar{k}_M = -\frac{D}{h}(4p\epsilon s)^{1/3}\frac{\pi\bar{\alpha}^2}{s}\left[\frac{Ai'(\bar{\alpha}^2)}{Ai(\bar{\alpha}^2)}\left[\frac{1}{\pi\bar{\alpha}^2} + Hi(\bar{\alpha}^2) - Bi(\bar{\alpha}^2)\right] - Hi'(\bar{\alpha}^2) + Bi'(\bar{\alpha}^2)\right], \tag{A.8}$$

or in terms of the modified Bessel functions of the third kind, $K_\nu(\zeta)$, where $\zeta = 2\alpha^3/3s$.:

$$\bar{k}_M = \frac{D}{h}(4p\epsilon)^{1/3}\frac{\alpha}{s}\left[\frac{K_{\frac{2}{3}}(\zeta) + \int_0^\zeta K_{\frac{1}{3}}(t)\,dt - \frac{\pi}{\sqrt{3}}}{K_{\frac{1}{3}}(\zeta)}\right]. \tag{A.9}$$

As we did when we calculated k_M for the dissociation case, we use an expansion of the form:

$$\frac{K_{\frac{2}{3}}(\zeta) + \int_0^\zeta K_{\frac{1}{3}}(t)\,dt - \frac{\pi}{\sqrt{3}}}{K_{\frac{1}{3}}(\zeta)} = \sum_{m=1}^{\infty} b_m \zeta^{(2m-3)/3}. \tag{A.10}$$

The first 20 coefficients of b_m are listed in Table 1. Substituting the expansion into Eq. (A.9) we have:

$$\bar{k}_{\mathrm{M}} = \frac{D}{h}(4p\epsilon)^{1/3}\alpha \sum_{m=1}^{\infty} b_m \left(\frac{2\alpha^3}{3}\right)^{(2m-3)/3} s^{-2m/3}. \tag{A.11}$$

Finally, we obtain $k_{\mathrm{M}}(x)$ by taking the inverse Laplace transform of Eq. (A.11):

$$k_{\mathrm{M}}(x) = \frac{D}{h}(4p\epsilon)^{1/3}\alpha \sum_{m=1}^{\infty} \frac{b_m}{\Gamma\left(\frac{2m}{3}\right)} \left(\frac{2\alpha^3}{3}\right)^{(2m-3)/3} x^{(2m-3)/3}. \tag{A.12}$$

When $\alpha \to 0$ Eq. (A.12) reduces to Eq. (33) and we recover the result when no soluble receptor is present.
From Eq. (A.12) we obtain $\langle k_{\mathrm{M}} \rangle$ by averaging over the length of the sensor surface.

$$\langle k_{\mathrm{M}} \rangle = \frac{D}{h}(4p\epsilon)^{1/3}\alpha \sum_{m=1}^{\infty} \frac{b_m}{\Gamma\left(\frac{2m+3}{3}\right)} \left(\frac{2\alpha^3}{3}\right)^{(2m-3)/3}. \tag{A.13}$$

Appendix B: Summary of data fitting procedure

The procedure outlined below is used to determine the dissociation constant, k_{d}, from Biacore experiments where soluble receptor (the soluble form of the molecule that is coupled to the sensor surface) is present during the dissociation phase (see Fig. 6). First, for each dissociation curve, corresponding to different soluble receptor concentrations, S_{T}, the halflife for dissociation, $t_{1/2}$ is determined. Then a nonlinear least squares fit of the data is done using the following expression for $t_{1/2}$ (see Fig. 7):

$$t_{1/2} = \frac{\ln 2}{k_{\mathrm{d}}}\left(1 + \delta(1 - b_0/(2\ln 2)) + c_1\delta^2 + c_2\delta^3 + c_3\delta^4\right) \tag{B.1}$$

where

$$\delta = \bar{\delta}\frac{R_{\mathrm{T}}}{R_0}\left(\frac{1 + p_4\alpha + p_5\alpha^2 + \alpha^3}{0.807594 + p_1\alpha + p_2\alpha^2 + p_3\alpha^3 + \alpha^4}\right) \tag{B.2}$$

and

$$\alpha = \bar{\alpha}(S_{\mathrm{T}}/S_0)^{1/2}. \tag{B.3}$$

There are four parameters, k_{d}, $\bar{\delta}$, b_0 and $\bar{\alpha}$, that are taken to be free. If equilibrium is achieved in the forward kinetics in all experiments, there is only a single b_0 parameter. If with different surface receptor concentrations different amounts of binding are achieved when dissociation is initiated, there is a different b_0 for each surface concentration as in Fig. 7. In fitting the data b_0 should be held between

zero and one. For example, one can set $b_0 = \gamma^2/(1+\gamma^2)$ and take γ as the free parameter instead of b_0. The quantity $S_0 = 1$, where the units of S_0 are the same as those of S_T. If data is being analyzed for a series of experiments using different surface receptor concentrations then R_0 is set equal to the lowest RU value. ($\bar{\alpha}$ and $\bar{\delta}$ and lumped parameters given by Eq. (46).) The additional parameters are held constant during the fitting at the following values: $c_1 = 9.55924 \times 10^{-3}$, $c_2 = -2.41944 \times 10^{-4}$, $c_3 = 1.87714 \times 10^{-6}$, $p_1 = 1.24240$, $p_2 = 1.41371$, $p_3 = 1.045663$, $p_4 = 1.55924$, and $p_5 = 1.00918$.

References

Abramowitz, M., Stegun, I.A. (Eds.), 1964. Handbook of Mathematical Functions. National Bureau of Standards, Washington, DC.

Bondeson, K., Frostell-Karlssonk, A., Fägerstam, L., Magnusson, G., 1993. Lactose repressor-operator DNA interactions: Kinetic analysis by a surface plasmon resonance biosensor. Anal. Biochem. 214, 245–251.

Brody, J.P., Yager, P., Goldstein, R.E., Austin, R.H., 1996. Biotechnology at low Reynolds numbers. Biophys. J. 71, 3430–3441.

Day, Y.S.N., Baird, C.L., Rich, R.L., Myszka, D.G., 2002. Direct comparison of binding equilibrium, thermodynamic, and rate constants determined by surface- and solution-based biophysical methods. Protein Sci. 11, 1017–1025.

Edwards, D.A., 2001. The effect of a receptor layer on the measurements of rate constants. Bull. Math. Biol. 63, 301–327.

Edwards, D.A., 2004. Refining the measurement of rate constants in the BIAcore. J. Math. Biol. 49, 272–292.

Efforon B., Tibshirani, R., 1986. Bootstrap methods for standard errors, confidence intervals, and other measures of statistical accuracy. Stat. Sci. 1, 54–77.

Ekebjaerg, L. and Justesen, P., 1991. An explicit scheme for advection-diffusion modeling in two dimensions. Comput. Methods Appl. Mech. Eng. 88, 287–297.

Garland, P.B., 1996. Optical evanescent wave methods for the study of biomolecular interactions. Q. Rev. Biophys. 29, 91–117.

Glasser, R.W., 1993. Antigen–antibody binding and mass transport by convection and diffusion to a surface: a two-dimensional computer model of binding and dissociation kinetics. Anal. Biochem. 213, 152–161.

Goeddel, D.V., Yansura, D.G., Caruthers, M.H., 1977. Binding of synthetic lactose operator DNAs to lactose repressors. Proc. Natl. Acad. Sci. U.S.A. 74, 3292–3296.

Goldstein, B., Coombs, D., He, X., Pineda, A.R., Wofsy, C., 1999. The influence of transport on the kinetics of binding to surface receptors: application to cells and BIAcore. J. Mol. Recognit. 12, 293–299.

Goldstein, B., Posner, R.G., Torney, D., Erickson, J., Holowka, D., Baird, B., 1989. Competition between solution and cell surface receptors for ligand: The dissociation of hapten bound to surface antibody in the presence of solution antibody. Biophys. J. 56, 955–966.

Johnssonm B., Lofas, S., Lindquist, G., 1991. Immobilization of proteins to a carboxy methyldextran-modified gold surface for biospecific interaction analysis in surface plasmon resonance sensors. Anal. Biochem. 198, 268–277.

Jones, S., Rose-John, S., 2002. The role of soluble receptors in cytokine biology: The agonistic properties of the sIL-6R/IL-6 complex. Biochim. Biophys. Acta 1592, 251–264.

Karlsson, R., Fält, A., 1997. Experimental design for kinetic analysis of protein–protein interactions with surface plasmon resonance biosensors. J. Immun. Methods 200, 121–133.

Lok, B.K., Cheng, Y.-L., Robertson, C.R., 1983. Protein adsorption on crosslinked polydimethylsiloxane using total internal reflection fluorescence. J. Colloid Interface Sci. 91, 104–116.

Mason, T., Pineda, A.R., Wofsy, C., Goldstein, B., 1999. Effective rate models for the analysis of transport-dependent biosensor data. Math. Biol. Sci. 159, 123–144.

Myszka, D.G., He, X., Dembo, M., Morton, T.A., Goldstein, B., 1998. Extending the range of rate constants available from BIACORE: Interpreting mass transport influenced binding data. Biophys. J. 75, 583–594.

Pattnaik, P., 2005. Surface Plasmon Resonance: Applications in understanding receptor-ligand interaction. Appl. Biochem. Biotech. 126, 79–92.

Rich, R.L., Myszka, D.G., 2000. Advances in surface plasmon resonance biosensor analysis. Curr. Opin. Biotech. 11, 54–61.

Rose-Hohn, S., Heinrich, P.C., 1994. Soluble receptors for cytokines and growth factors: generation and biological function. Biochem. J. 300, 281–290.

Segel, L.A., Slemrod, M., 1989. The quasi-steady state assumption: A case study in perturbation. SIAM Rev. 31, 446–477.

Wofsy, C., Goldstein, B., 2002. Effective rate models for receptors distributed in a layer above a surface: application to cells and BIACORE. Biophys. J. 82, 1743–1755.

Yansura, D.G., Goeddel, D.V., Cribbs, D.L., Caruthers, M.H., 1977. Studies on gene control regions. 3. Binding of synthetic and modified synthetic lac operator DNAs to Lactose repressor. Nucleic Acids Res. 4, 723–737.